Analysis of Heat Distribution for Different Types of Traveling Wave Induction Heater Based On 3D FEM

Prof. A. K. Al-Shaikhli, Asst. Prof. Abdul-Rahim T. Humod, Fadhil A. Hasan*

Abstract— Traveling Wave Induction Heater (TWIH) is very promising and attractive tool in the field of heating flat materials. Analytical methods are more convenient for the integral parameters determination and analysis, while the numerical ones are more universal and particularly useful for investigating the induced current and power distributions. This paper presents the numerical analysis of such system based on 3D Finite Element Analysis (FEAs), taking into account the nonlinearity of the workpiece permeability. The available 3D finite element program ANSYS R15 PC codes are used to simulate different TWIH entities and geometries. The presented 3D simulations verify the performances of the selected methods, and gives comparison between the distributions of magnetic flux, eddy current, power densities, and temperature along the position of the strip for different TWIH systems. The presented 3D analysis provides a powerful solution of the TWIH electromagnetic problem.

Index Terms— traveling wave induction heating, 3D analysis, eddy current, power density, and temperature distribution, induction heating.

1 INTRODUCTION

Heating process of strip material is very important in industry. Traditional longitudinal method and single-phase transverse flux technology are inadequate to meet the ever increasing demand on quality performance in regard to temperature uniformity on the work strips, especially on thin and long strips. Among the multiphase systems being developed recently, the Traveling Wave Induction Heater process is potentially very promising and attractive [1]. Traveling wave induction heaters have particular features which make them attractive for application to some heating processes in industry. Among them it can be mentioned that [2]:
The use of the power frequency for heating flat materials.
The mechanical strength and the protection for the coils given by the ferromagnetic core.
The possibility of avoiding power unbalance circuits since a nearly balanced poly-phase load is presented to the supply.
Reducing vibrations and noise of the inductor-load system due to the electrodynamics forces and obtaining switch power distributions in the load by convenient arrangements of the winding.

The most important features of the TWIH that it can get more uniform temperature field distribution. There are many factors which affect the performance of the inductors, like the winding arrangement, the edge-effects, the slots effects, the relative position of the upper and lower inductor, etc [3]. The traveling wave induction heaters, however, are not fully appreciated with respect to their main advantages and possible industrial applications.
There are a few types of winding arrangement and structure of the TWIH system in the literature. This paper represents these types and describes the performance, heating uniformity and eddy current distribution over the workpiece. The three-dimensional (3D) Finite-Element Analysis (FEAs) has now become feasible in practical applications, not only for steady-state field analysis, but also for transient performance study of induction heater [4]. This work used 3D FEAs in order to study the performance of different types of TWIH systems.

* *Electrical Engineering Department, University of Technology, Baghdad, Iraq. E-mail: fadhil.a.hassan@gmail.com.*

2 MODEL ANALYSIS

The mathematical model of the electromagnetic phenomena is based on Maxwell's equations and wave propagation theory, the four equations are as the following:

$$\nabla \times \bar{H} = \bar{J} + \partial \bar{D}/\partial t \quad (1)$$

$$\nabla . \bar{B} = 0 \quad (2)$$

$$\nabla \times \bar{E} = -(\partial \bar{B}/\partial t) \quad (3)$$

$$\nabla . \bar{D} = \rho \quad (4)$$

Where: $\bar{H}$ is the magnetic field intensity, $\bar{B}$ is the magnetic field density, $\bar{E}$ is the electric field intensity, $\bar{D}$ is the electric displacement vector, and $\bar{J}$ is the current density, ρ is volume charge density.
Since $\bar{D} = \varepsilon \bar{E}$ and $\bar{J} = \sigma \bar{E}$
Where: ε is the permittivity, σ is the conductivity.
Rewrite (1):

$$\nabla \times \bar{H} = \sigma \bar{E} + \varepsilon(\partial \bar{E}/\partial t) \quad (5)$$

For sinusoidal magnetic field:

$$\nabla \times \bar{H} = (\sigma + j\varepsilon\omega)\bar{E} \quad (6)$$

For super conducting materials:

$$\sigma \gg \varepsilon\omega \quad \rightarrow \quad \nabla \times \bar{H} = \sigma \bar{E} = \bar{J}$$

Since $\bar{B} = \nabla \times \bar{A}$ where $\bar{A}$ is the magnetic vector potential, then the mathematical model of the eddy current results can be described by means of the complex magnetic vector potential $\bar{A}$ and a complex scalar potential φ (where φ is the

magnetic scalar potential H= -∇φ):

$$\bar{J} = -\sigma(\partial\bar{A}/\partial t + \nabla\,\partial\bar{\varphi}/\partial t) + \bar{J}_s \qquad (7)$$

Where: $\bar{J}_s$ is the impressed exciting current density.

It can be seen from (7) that the current density in the strip is proportional to the rate of change of the magnetic flux and the field intensity, so magnetic field which is inducted by TWIH can create different vortex effect in the strip [5].

3 Traveling Wave Inductors Types

Basically there are two main types of TWIH systems; single-side and double side. This paper focuses on the double side TWIH systems because they are the most used heater, while; the single side is rarely used because of their low efficiency and low heat transfer. The double sides TW Inductors have two main types: slotted TW Inductor and slotless TW Inductor.

3.1 Slotted TW Inductors

In the traditional TWIH the efficient airgap between the coil and load in slotted TWIH is longer than airgap between the teeth and load. It is obvious that "g1" is longer the "g" in fig1. Therefore, the magnetic field density will be more intensive below the tooth position than the air position in the strip. Winding arrangement could affect the choice of suitable power supply and the temperature distribution on the surface of the strip [5].

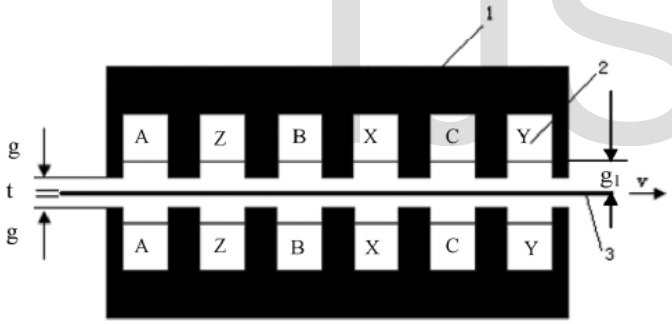

Fig.1. Traditional TW winding arrangement

Where: 1-yoke, 2-exciting winding, 3-moving metal strip, g-airgap between winding and strip, v-strip movement direction, g1-effective airgap between heater and load, t-strip thickness.

3.1.1 Winding Arrangement:

There are two types of winding arrangement; short bitch and long bitch. H. Tomita, et al [6] show that the heating range in the short pitch coil is wide and better than the full bitch coil. Nevertheless, they proved that the thermal distribution is more uniform than the full pitch coil also the thermal rising time in short pitch coil is shorter than in full pitch coil. Fig. 2 shows the winding distribution of the short-pitch coil.

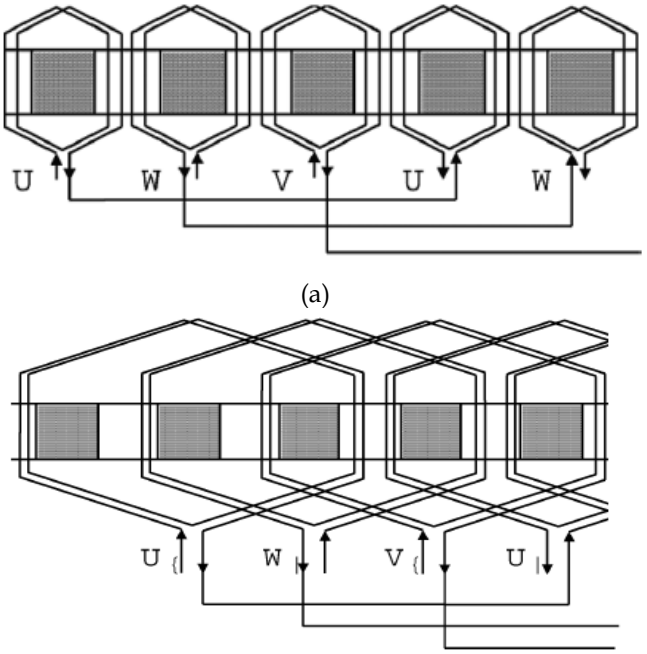

Fig.2. a) Short pitch winding, b) Long pitch winding

A. Ali, et al [7] propose up-down mode and the left-right mode coil's different heating effects. For the up-down mode coil shown in Fig. 3, its power distributions in the strip are particularly uniform and are almost the same for current and voltage supply. In this system six power peaks are presenting along the center of the sheet in the movement direction and the power pulsations are almost equal.

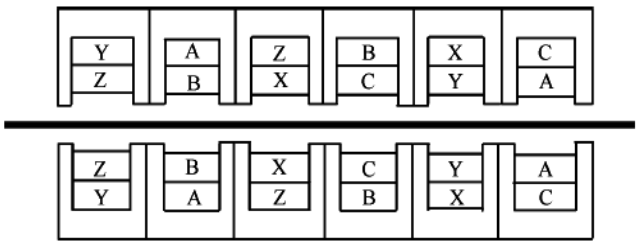

Fig.3. Up-down winding distribution

The left-right mode coil in Fig. 4 get a non-uniform power distribution in the strip, and three power peaks are presenting along the center of the sheet in movement direction.

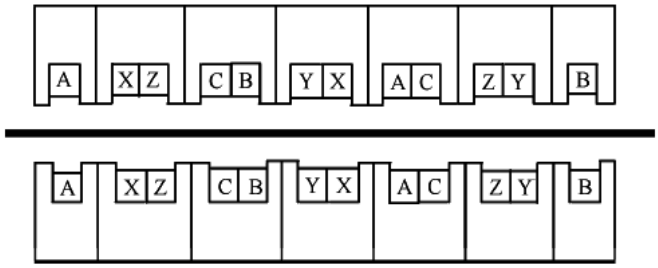

Fig.4. Left-right winding distribution

F. Dughiero, et al [2] has introduced the structure shown in Fig. 5, its current coils with current phase shift 30 degrees for adjacent windings. In this system twelve power peaks are presenting along the center of the sheet in the movement direction and the power density with very much reduced tooth pulsations. The length of this system is much longer than the classic TWIH system. But this structure cannot be well applied, because in this case a more complex power supply should be prepared.

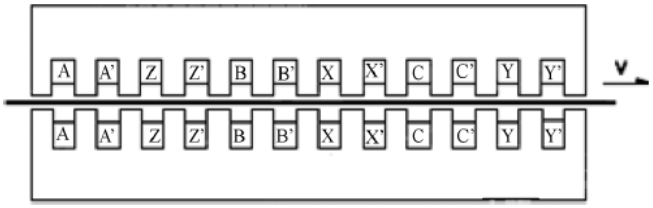

Fig.5. Distribution winding arrangement

3.1.2 Crossed Traveling Wave Induction Heater

The crossed TWIH system C-TWIH proposed by S. L. Ho, et al [1] as shown in fig. 6 they show that the C-TWIH has more uniform and concentrated eddy current density distribution. This is because the C-TWIH system exploits a three phase induction heater with crossed yoke arrangement, and the magnetic flux generated by each phase are interacting and complementing each other to compensate for the weak magnetic areas of each phase.

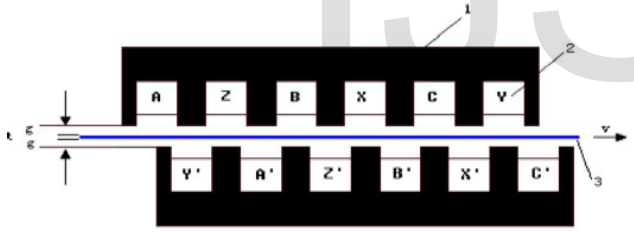

Fig.6. Schematic of the double-sided C-TWIH system

3.1.3 Slot Wedges TW Induction Heater

Slot wedges traveling wave induction heater was proposed by Junhua Wang, et al [4]. Fig. 7 shows the SW-TWIH system which has the structure of the typical TWIH with distributed windings and there are magnetic slot wedges (SW) in each coil. Two linear inductors and thirty three coils are installed on the opposite sides of the strip along the direction of movement to generate the traveling wave. Due to the thickness of the interposing refractory materials, there is a relatively large air gap between the inductor and the strip. Moreover, for improving the system, the authors proposed a nonmagnetic strip fitted in middle of SW. The proposed SW enabling the magnetic fluxes generated by each phase to interact and complement with each other and compensate for the weak magnetic areas so as to generate more uniform and concentrated eddy-current density lead to more homogeneous temperature distribution.

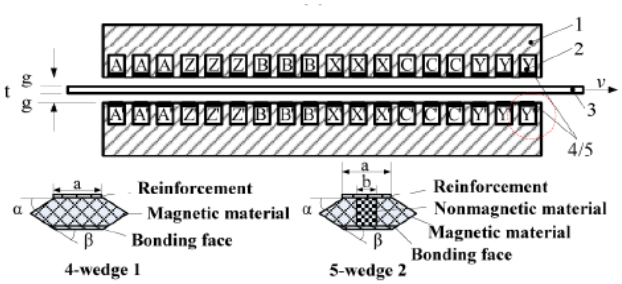

Fig.7. (1–magnetic yoke; 2–exciting windings; 3–load metal sheet; t-strip thickness; g-airgap between inductor and load; v-strip movement velocity. Initial phase angle: A–X and A'–X' =0°, B-Y and B'–Y'=-120°, C-Z and C'-Z'=-240°). SW-TWIH (wedge 1) and improved SW-TWIH (wedge 2)

3.1.4 Distributed Vernier Traveling Wave Induction Heater

A traveling wave induction heating system with distributed winding and vernier structure (DV-TWIH) was proposed by Tunhua Wang, et al [8]. This system is specially designed to address the inhomogeneous eddy current density problem that dominates the pattern of thermal distribution on the surface of work as shown in fig. 8. The proposed double-layer vernier combined enables the magnetic flux generated by each phase to interact and complement each other to compensate for local weak magnetic fluxes in order to generate more uniform and concentrated eddy current density and temperature distribution in the work piece.

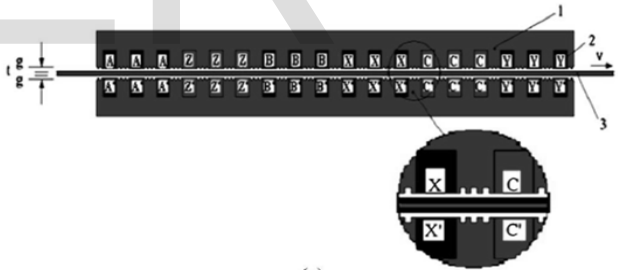

Fig.8. (1–magnetic yoke; 2–exciting windings; 3–load metal sheet; t-strip thickness; g-airgap between inductor and load; v-strip movement velocity. Initial phase angle: A–X and A'–X' =0°, B-Y and B'–Y'=-120°, C-Z and C'-Z'=-240°). Schematic of a typical double-side DV-TWIH system

3.2 Slotless TW Induction Heating

There are main two drawbacks of the traditional TW inductors first; the induced magnetic field density below the tooth position will be bigger than the air position in the strip. Second; that some of the magnetic lines do not pass through the load. This will affect the efficiency of the power transferred from the coils to the load. For that's Lingling Pang, et al [3] propose slotless model to reduce the slots effects as shown in fig. 9. The simulation results prove that this slotless TW model could obtain an ideal eddy current density distribution in the metal strip. The main

characteristics of the slotless model are the absence of slots and teeth on the surface of magnetic yoke, and the real coils are considered as current sheets. Virtually this study introduces some unrealistically over-simplified and practical assumptions for such proposed current sheet on a magnetic yoke without slots [4].

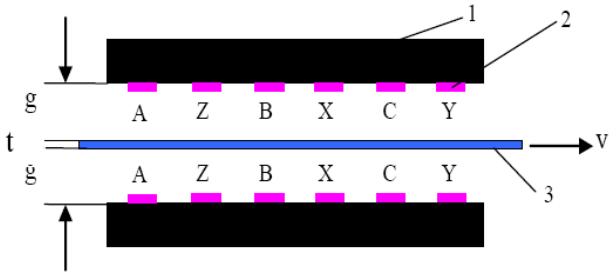

Fig.9. Schematic of a double-side slotless TW inductor [1- the yoke, 2-exciting windings, 3- moving metal strip, t-strip thickness, g-airgap between inductor and load, v-strip movement direction].

4 3D Transient Analysis

For transient performance, such as flux density, eddy current and temperature distributions, the traditional methods don't give accurate results as expected due to skin effects on the solid pole surfaces and serious magnetic nonlinearities. With the advent of powerful computing workstations, two-dimensional (2D) and three-dimensional (3D) finite element analysis (FEAs) have now become feasible in practical applications, not only for steady-state field analysis, but also for transient performance study of induction heaters [1], [9]. For complicated TWIHs, transient 3D FEA study of the flux density, eddy current and temperature distributions is however computationally expensive and hence not feasible for industrial applications because of the complex 3D meshing process and excessively long solution time.

5 Simulation Results

In order to investigate the performance of different types of TWIH systems with a suitable accuracy factor, double side nonlinear inductors on the opposite sides of the strip is used. The nonlinearity of the B-H curve of the steel core is taken in account during the 3D analysis. Slots perpendicular to the direction of the movement, and a relatively large air gap due to the thickness of the refractory material interposed between the inductor and the strip. The parameters of the used system for different types are given in Table 1.

TABLE 1
SYSTEM PARAMETERS

Heater	Length	1.36 m
	Height	0.1 m
	Width	0.125
	Relative Permeability	Steel B-H curve
	No. of phases	3
	Excited current density (J)	10 MA/m^2
	Frequency	50 Hz
	Air gap	.005 m
Strip (Aluminum)	Length	1.6 m
	Width	0.125 m
	Thickness	.008 m
	Resistivity (ρ)	2.82x10-8
	Relative Permeability	1
Thermal conditions	Ambient temperature	25 C^o
	Convection coefficient	100 W/(m^2.C)
	Thermal conductivity	50 W/(m.C)

The FEAs results of the 3D transient solutions are obtained by using programming codes of ANSYS R15. Fig. 10, 11, 12, and 13 shows sample of the simulation analysis for single layer, double layer, cross, and distributed TWIH systems at phase angle 180^o.

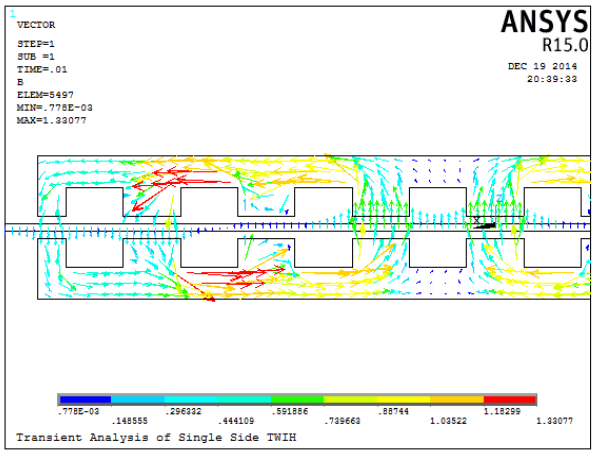

(a)

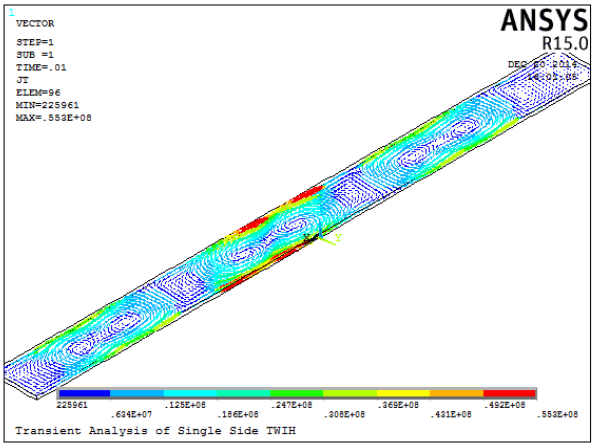

(b)

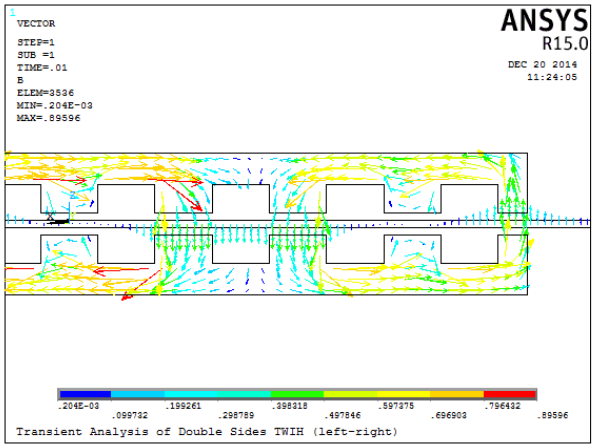

(a)

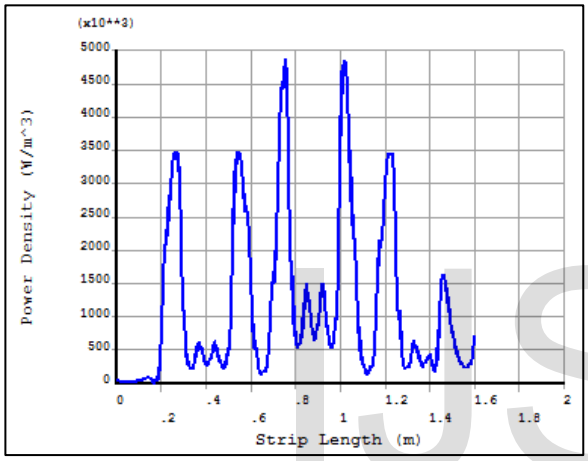

(c)

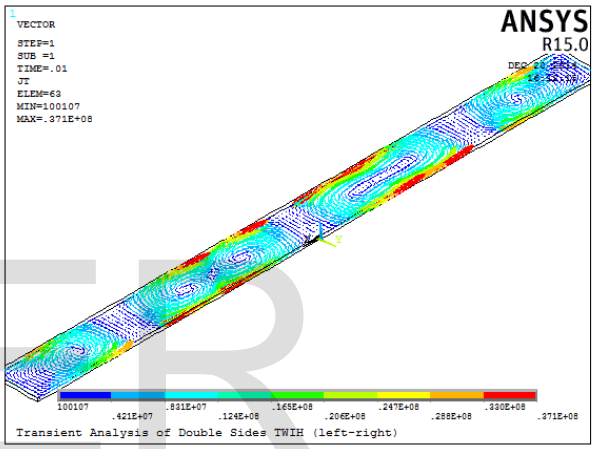

(b)

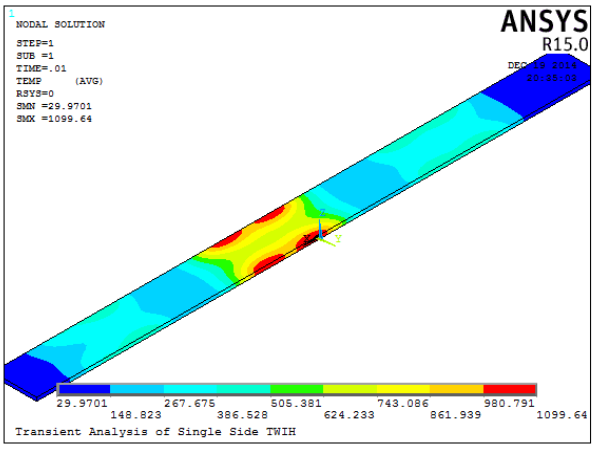

(d)

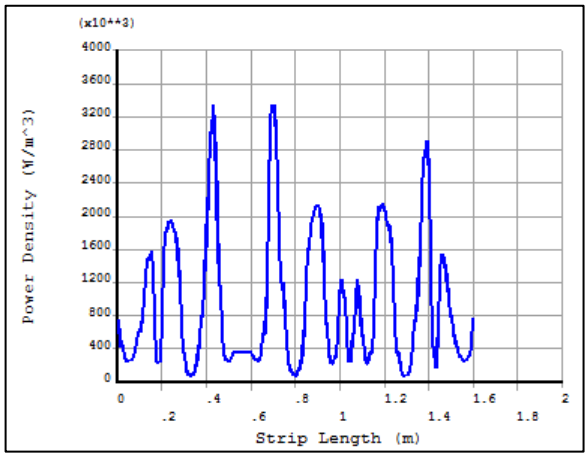

(c)

Fig. 10; a) Magnetic flux density, b) Eddy current, c) Power density and d) Temperature of the traditional single layer TWIH

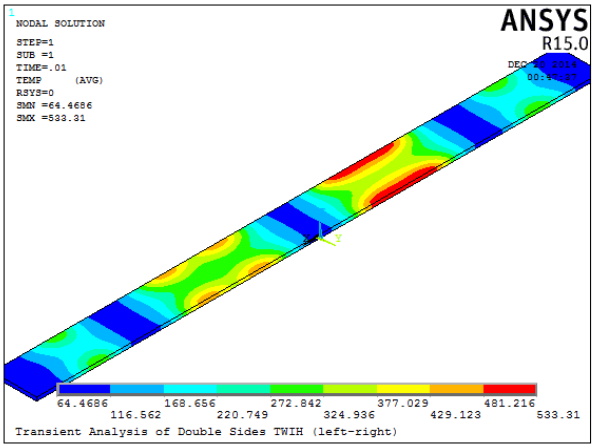

(d)

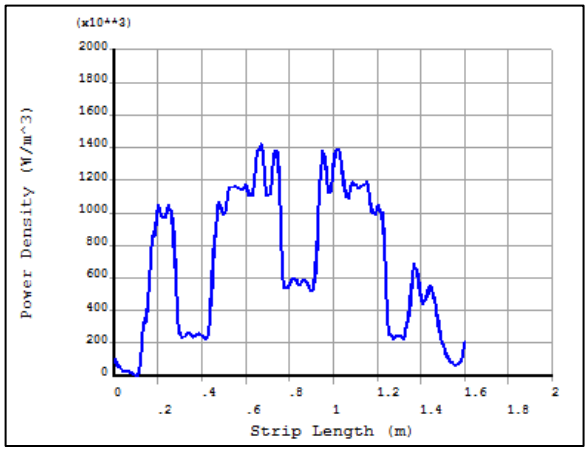

(c)

Fig. 11; a) Magnetic flux density, b) Eddy current, c) Power density and d) Temperature of the traditional double layers TWIH

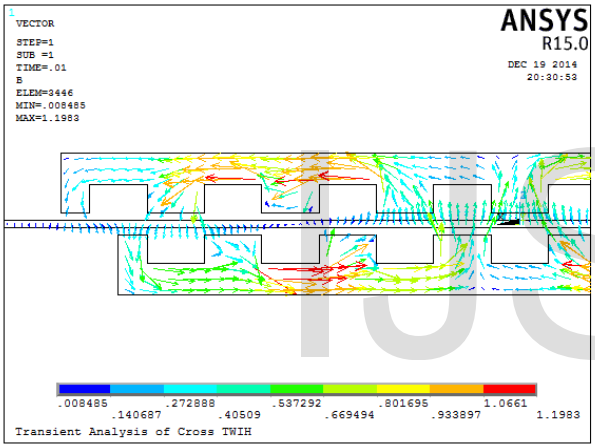

(a)

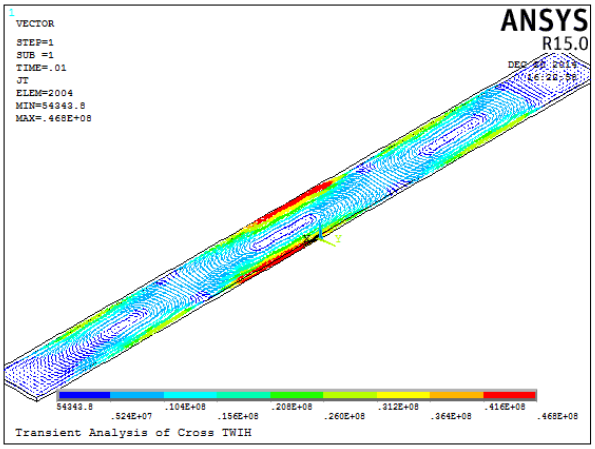

(b)

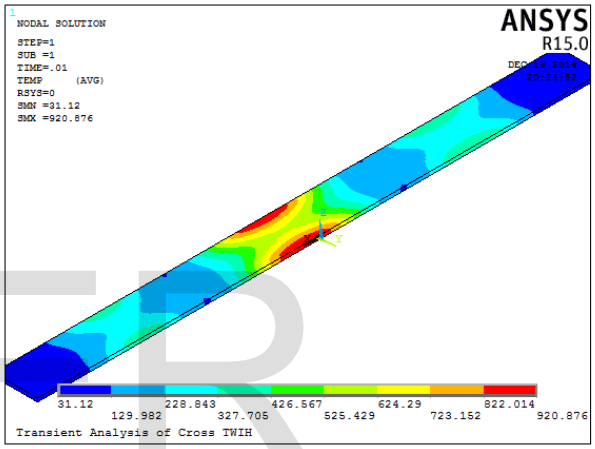

(d)

Fig. 12 a) Magnetic flux density, b) Eddy current, c) Power density and d) Temperature of the Cross TWIH

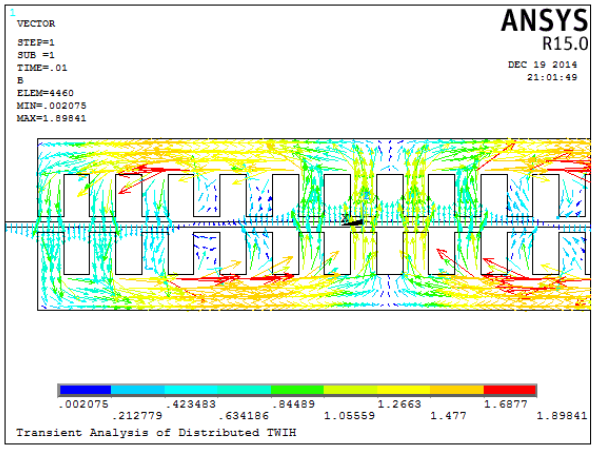

(a)

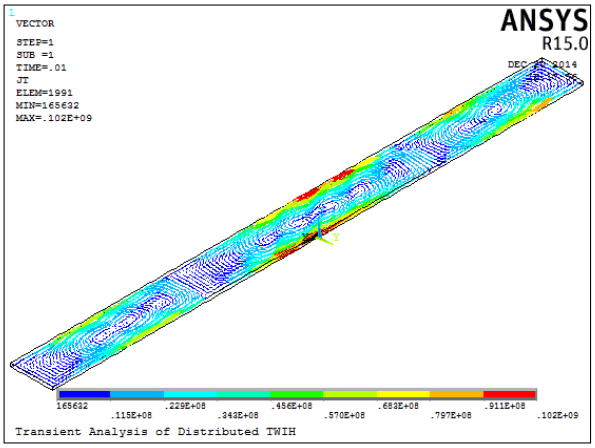

(b)

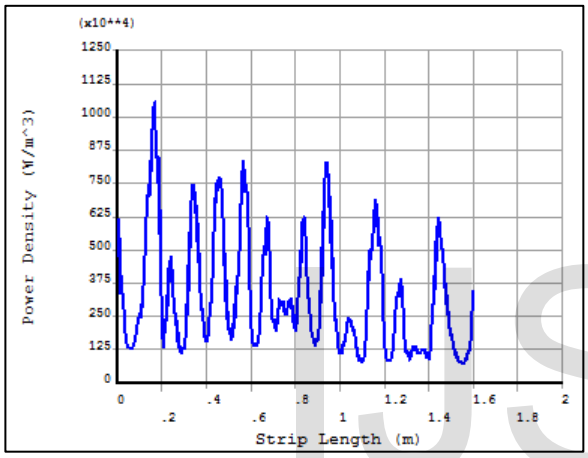

(c)

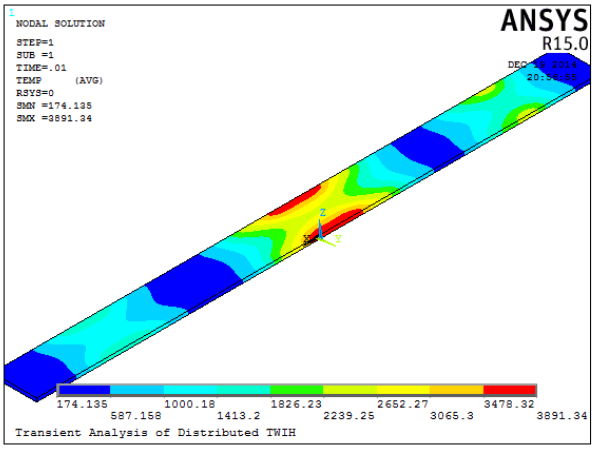

(d)

Fig. 13; a) Magnetic flux density, b) Eddy current, c) Power density and d) Temperature of the Distributed TWIH

The obtained results can be summarized in tables 2, 3, 4 and 5 for different types of TWIH:

TABLE 2
MAGNETIC FLUX DENSITY (T)

TWIH Method	Min.	Max.	Average
Single Layer	7*10-3	1.33	0.669
Double Layer (left-right)	2*10-3	0.9	0.451
Double Layer (upper-lower)	2*10-3	1.05	0.526
C-TWIH	8*10-3	1.2	0.604
D-TWIH	2*10-3	1.9	0.951
SW-TWIH	4*10-3	1.85	0.927
DV-TWIH	1*10-3	2.06	1.031

TABLE 3
EDDY CURRENT DENSITY (A/M^2)

TWIH Method	Min.	Max.	Average
Single Layer	$226*10^3$	$0.55*10^8$	$2.8*10^7$
Double Layer (left-right)	$100*10^3$	$0.37*10^8$	$1.9*10^7$
Double Layer (upper-lower)	$342*10^3$	$0.45*10^8$	$2.3*10^7$
C-TWIH	$54*10^3$	$0.47*10^8$	$2.4*10^7$
D-TWIH	$165*10^3$	$1*10^8$	$5*10^7$
SW-TWIH	$125*10^3$	$0.96*10^8$	$4.8*10^7$
DV-TWIH	$105*10^3$	$0.91*10^8$	$4.6*10^7$

TABLE 4
POWER DENSITY (W/M^3)

TWIH Method	Min.	Max.	Average
Single Layer	7*10-3	1.33	0.669
Double Layer (left-right)	2*10-3	0.9	0.451
Double Layer (upper-lower)	2*10-3	1.05	0.526
C-TWIH	8*10-3	1.2	0.604
D-TWIH	2*10-3	1.9	0.951
SW-TWIH	4*10-3	1.85	0.927
DV-TWIH	1*10-3	2.06	1.031

TABLE 5
TEMPERATURE (C^O)

TWIH Method	Min.	Max.	Average
Single Layer	29.9	1099	564.5
Double Layer (left-right)	64.4	533.3	298.9
Double Layer (upper-lower)	87	756.8	421.9

C-TWIH	31.1	920.8	476
D-TWIH	174	3891	2033
SW-TWIH	134	3885	2010
DV-TWIH	170	3729	1950

6 Conclusion

In this paper, various types of traveling wave inductors for the continuous heating of thin aluminum strip has been analyzed. The 3D finite element simulation results certified the performances of such systems as shown in figures 10, 11, 12 and 13. A comparison between the distributions of magnetic flux, eddy current, power densities, and temperature along the position of the strip for different TWIH systems, can be shown in table II. The presented 3D analysis gives a powerful solution of the TWIH electromagnetic problem. Obviously, the analysis study shows that the highest power density and uniform temperature distribution obtained in the distributed, slot wedge and vernier TWIH systems than the other methods. Moreover, the number of maximum power peaks is grater in the distributed winding than other methods.

References

[1] S. L. Ho, Junhua Wang, W.N. Fu, and Y. H. Wang," A Novel Crossed Traveling Wave Induction Heating System and Finite Element Analysis of Eddy Current and Temperature Distributions", IEEE Transactions On Magnetics, Vol. 45, No. 10, October 2009.

[2] F. Dughiero, S. Lupi, V. Nemkov, P. Siega, "Travelling Wave Inductors for the Continuous Induction Heating of Metal Strips" 1994 IEEE.

[3] Lingling Pang, Youhua Wang, Tanggong Chen, "Analysis of Eddy Current Density Distribution in Slotless Traveling Wave Inductor",

[4] Junhua Wang, S. L.Ho, W.N. Fu, and Y. H. Wang, "Design and Analysis of a Novel Traveling Wave Induction Heating System With Magnetic Slot Wedges for Heating Moving Thin Strips", IEEE Transactions On Magnetics, Vol. 46, No. 6, June 2010.

[5] Lingling Pang, Youhua Wang, and Tanggong Chen, "New Development of Traveling Wave Induction Heating", IEEE Transactions On Applied Superconductivity, Vol. 20, No. 3, June 2010.

[6] H. Tomita, T. Sekine, and S. Obata, "Induction heating using traveling magnetic field and three-phase high-frequency inverter," in The 11th European Conference on Power Electronics and Applications, 2005, Dresden, Germany, September 11–14, 2005, pp. 1–6.

[7] A. Ali, V. Bukanin, F. Dughiero, S. Lupi, and V. Nemkov et al., "Simulation of multiphase induction heating systems," in IEE Conference Publication, 1994, vol. 38, no. 4, pp. 211–214.

[8] Junhua Wang, Youhua Wang_, S. L.Ho, Xiaoguang Yang, W.N. Fu, and Guizhi Xu," Design and FEM Analysis of a New Distributed Vernier Traveling Wave Induction Heater for Heating Moving Thin Strips", IEEE Transactions On Magnetics, Vol. 47, No. 10, October 2011.

[9] Z. Wang, X. Yang, Y. Wang, and W. Yan, "Eddy current and temperature field computation in transverse flux induction heating equipment," IEEE Trans. Magn., vol. 37, no. 5, pp. 3437–3439, Sep. 2001.